Electronic Supporting Materials

S1. AIMD calculations:

The diffusion coefficient is related to the average mean square displacement (MSD) from molecular dynamics (MD) runs at each temperature *T* over a period of time (t), $\langle[\Delta \boldsymbol{r}(\boldsymbol{t})]^{\boldsymbol{2}}\rangle$, as

$$\boldsymbol{D} = \frac{\boldsymbol{1}}{\boldsymbol{2dt}}\langle[\Delta \boldsymbol{r}(\boldsymbol{t})]^{\boldsymbol{2}}\rangle,$$

where *d* is the dimensionality factor. Using the Arrhenius relation, $\boldsymbol{D} = \boldsymbol{D_0}\ \mathbf{exp}(-\frac{\boldsymbol{E_a}}{\boldsymbol{k_B T}})$, one can derive $\boldsymbol{D_0}$ and $\boldsymbol{E_a}$ via plotting the logarithmic values of *D* against 1/*T*. Correction of the MSD from artefactual errors due to the periodic boundary condition is necessary for dependable AIMD evaluation of *D*, using the "unwrapped" trajectories to help achieve significant improvement in sampling statistics from limited simulation data typical for tractable AIMD runs.[1-5]

The ionic conductivity σ can then be derived using the Nernst−Einstein equation,[3, 6]

$$\boldsymbol{\sigma} = \frac{\boldsymbol{\rho z^2 F^2}}{\boldsymbol{RT}}\ \boldsymbol{D} = \frac{\boldsymbol{\rho z^2 F^2}}{\boldsymbol{RT}}\ \boldsymbol{D_0}\ \mathbf{exp}(-\frac{\boldsymbol{E_a}}{\boldsymbol{k_B T}})$$

where $\boldsymbol{\rho}$ is the molar density of diffusing alkali ions in the unit cell, z is the charge of alkali ions (+1 for Na^+), F and R are the Faraday's constant and the gas constant, respectively, D_0 is a constant, E_a is activation energy for diffusion, and k_B is the Boltzmann constant. The ionic conductivity is thus dictated by the diffusion process.

S2. Quasi-harmonic approximation in Gibbs free energy:

Gibbs free energy (G) of all phases belonging to the given compounds can be expressed as:

$$G = H - TS = E + pV - TS,$$

where H, E, p, V, T, and S represent the enthalpy, internal energy, pressure, volume, and entropy of the system, correspondingly.

Quasi-harmonic approximation is used for an approximation that introduces volume dependence of phonon frequencies as a part of anharmonic effect. A part of temperature effect can be included into total energy of electronic structure through phonon (Helmholtz) free energy at constant volume. Defined at a constant pressure by the transformation, Gibbs free energy can be expressed as:

$$G(T,P) = {}^{min}_{V}[U(V) + F_{phonon}(T;V) + pV],$$

where

$${}^{min}_{V}[function\ of\ V]$$

which means to find unique minimum value in the brackets by changing volume. By increasing temperature, the volume dependence of phonon free energy changes, then the equilibrium volume at temperatures changes. This is considered as thermal expansion under this approximation.

Formation energy for Na vacancy:

The formation energies of a Na vacancy in $Na_4S_{0.5}O_{0.5}I_2$ and $Na_3LiS_{0.5}O_{0.5}I_2$ are defined as

$$\Delta E_1 = E_{Na_4S_{0.5}O_{0.5}I_{2vac}} - (E_{Na_4S_{0.5}O_{0.5}I_2} - \mu_{Na}),$$
$$\Delta E_2 = E_{Na_3Li\ _{0.5}O_{0.5}I_{2vac}} - (E_{Na_3LiS_{0.5}O_{0.5}I_2} - \mu_{Na}).$$

where μ_{Na} is the chemical potential of Na (-1.31 eV). The calculated formation energies ΔE_1 and ΔE_2 are quite small (only around 0.013 eV/atom), indicating statistical readiness for the presence of vacancies in the materials due to energetic fluctuation (noticing that the thermal energy at room temperature is already about 0.025 eV).

Reference:

1. Y. Yu, Z. Wang and G. Shao, *J. Mater. Chem. A*, 2018, **6**, 19843-19852.
2. Z. Wang, H. Xu, M. Xuan and G. Shao, *J. Mater. Chem. A*, 2018, **6**, 73-83.
3. Z. Wang and G. Shao, *J. Mater. Chem. A*, 2017, **5**, 21846-21857.
4. H. Xu, Y. Yu, Z. Wang and G. Shao, *J. Mater. Chem. A*, 2019, **7**, 5239-5247.
5. M. V. Agnihotri, S. H. Chen, C. Beck and S. J. Singer, *J. Phys. Chem. B*, 2014, **118**, 8170-8178.
6. J. C. Bachman, S. Muy, A. Grimaud, H. H. Chang, N. Pour, S. F. Lux, O. Paschos, F. Maglia, S. Lupart, P. Lamp, L. Giordano and Y. Shao-Horn, *Chem. Rev.*, 2016, **116**, 140-162.

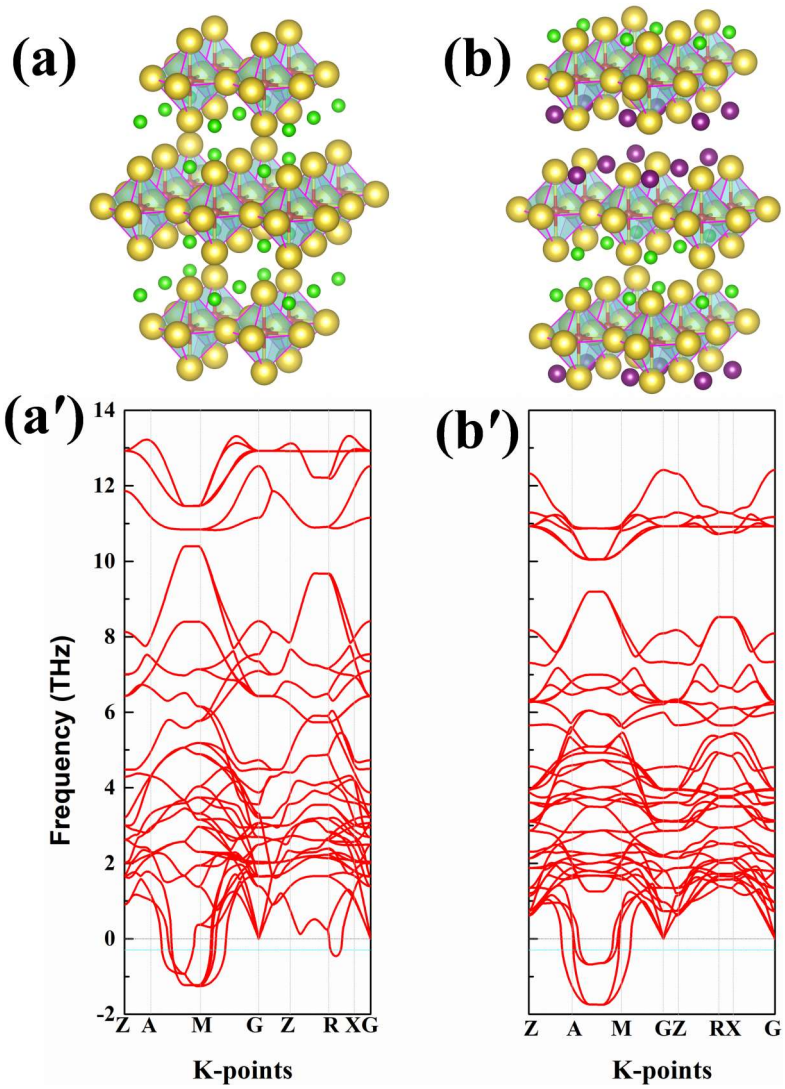

Fig. S1 Low-energy structures from USPEX global searching for (a)Na_4OCl_2_139 and (b)Na_4OICl_129. The associated phonon band structures are displayed in (a') and (b'), respectively.

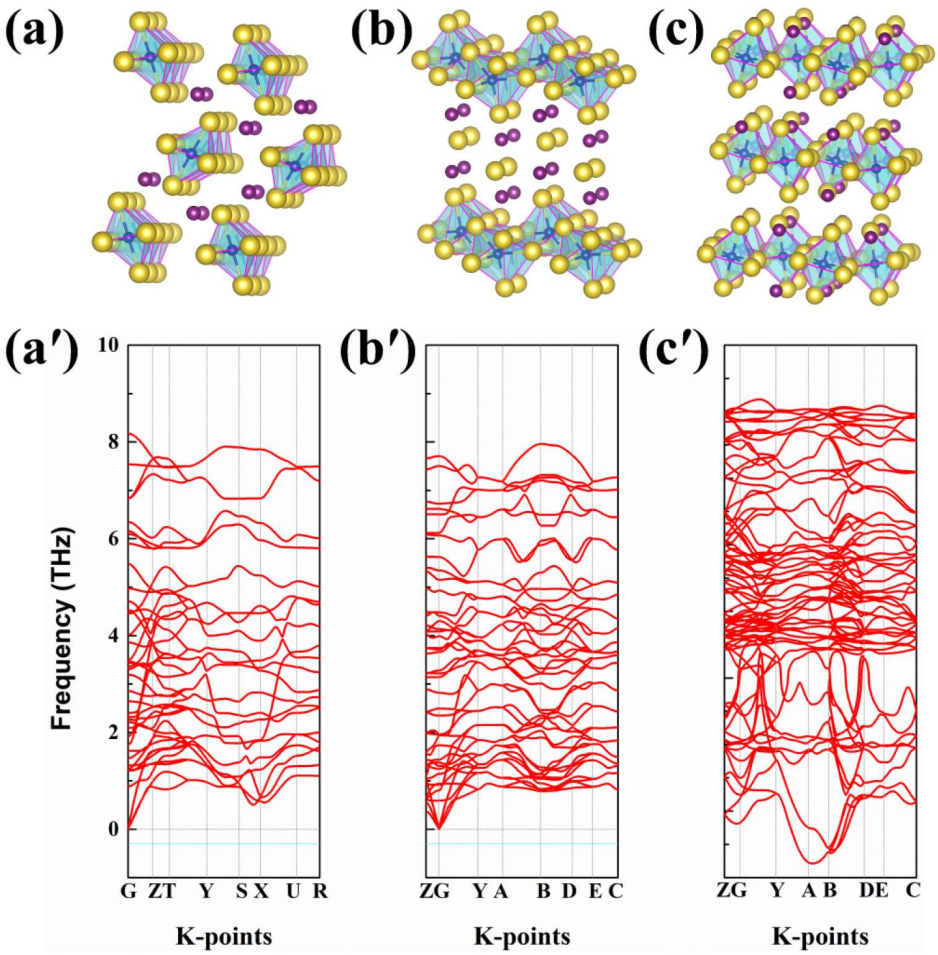

Fig. S2 Low energy structures from USPEX global searching for (a)Na_4SI_2_55, (b)Na_4SI_2_11 and (c)Na_4SI_2_64. The calculated phonon band structures are displayed in (a')-(c'), correspondingly.

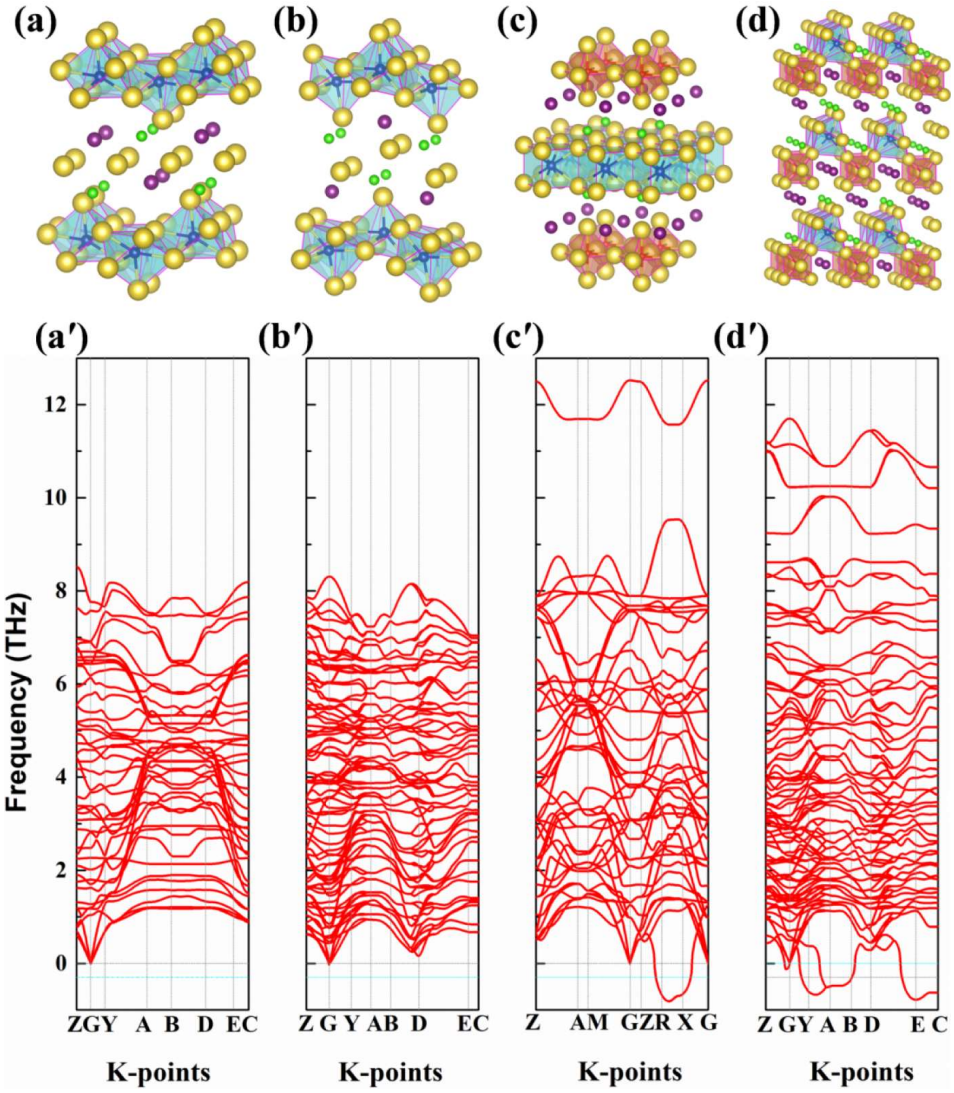

Fig. S3 The low-energy structures obtained from USPEX global searching for (a)Na_4SICl_12, (b)Na_4SICl_8, (c)$Na_4S_{0.5}O_{0.5}ICl\_123$, (d)$Na_4S_{0.5}O_{0.5}ICl\_8$. The corresponding calculated phonon band structures are displayed in (a')-(d').

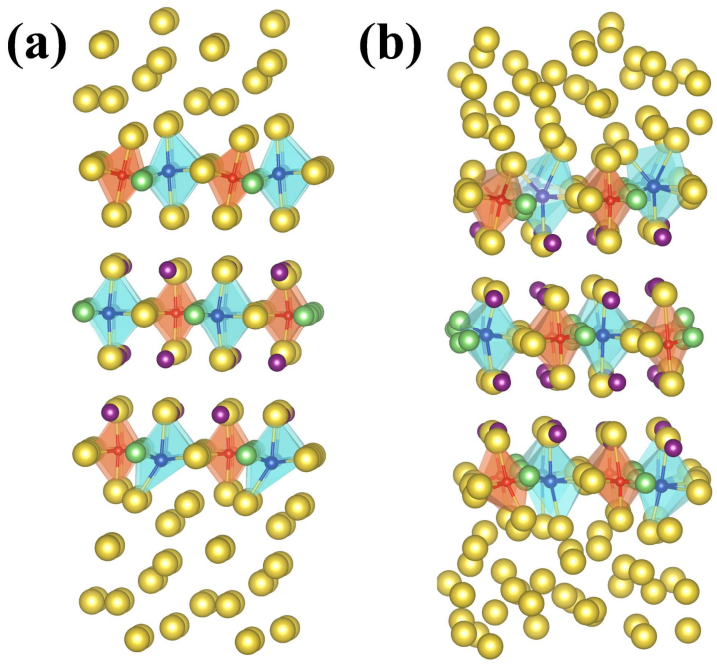

Fig. S4 Sandwich model of Na|$Na_3LiS_{0.5}O_{0.5}I_2$|Na: (a) before and (b) after AIMD simulation at 500 K.

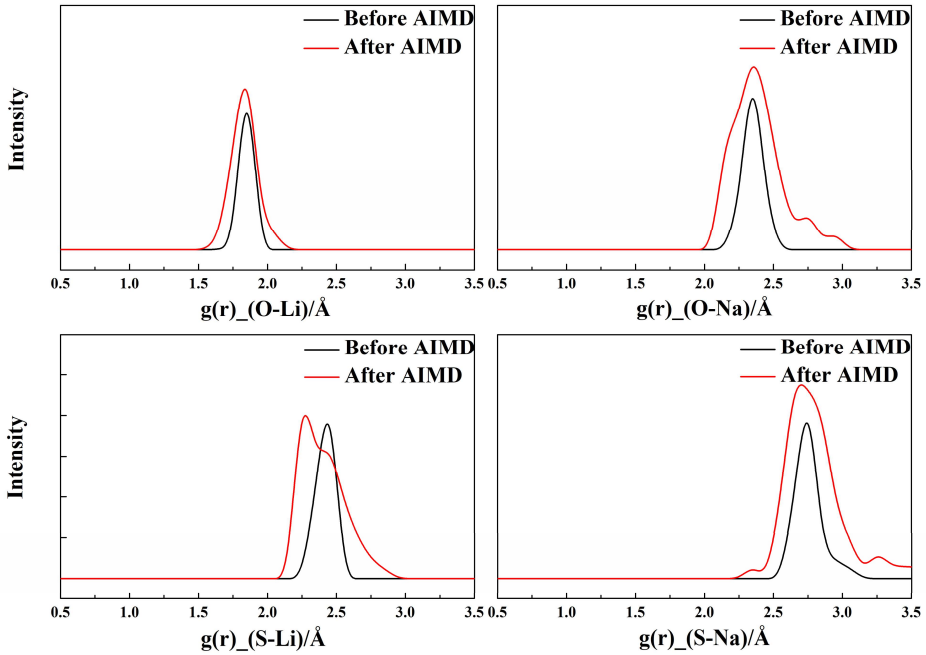

Fig. S5 Pair correlation functions (PCFs) for (a) O-Li, (b) O-Na, (c) S-Li and (d) S-Na bonds after AIMD simulation at 500 K.

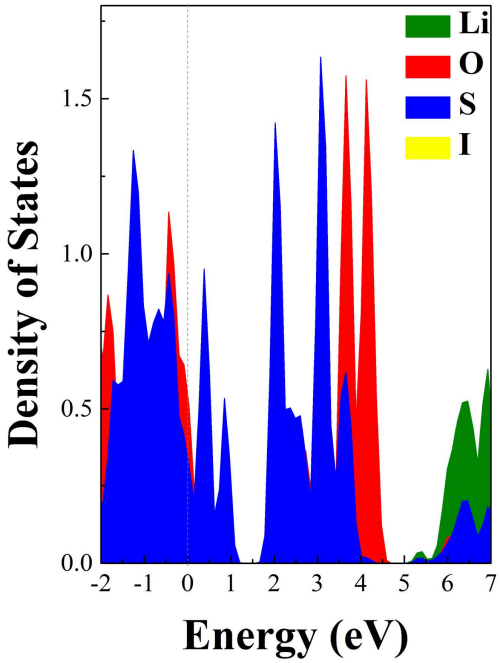

Fig. S6 Projected density of states for $LiS_{0.5}O_{0.5}I_2$.

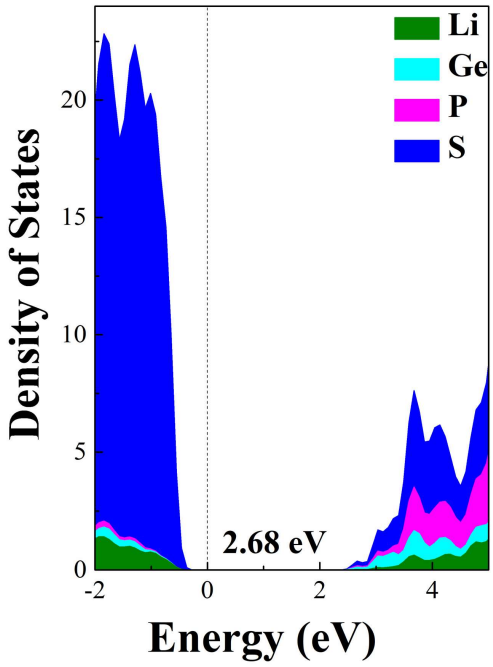

Fig. S7 The projected density of states for LGPS.

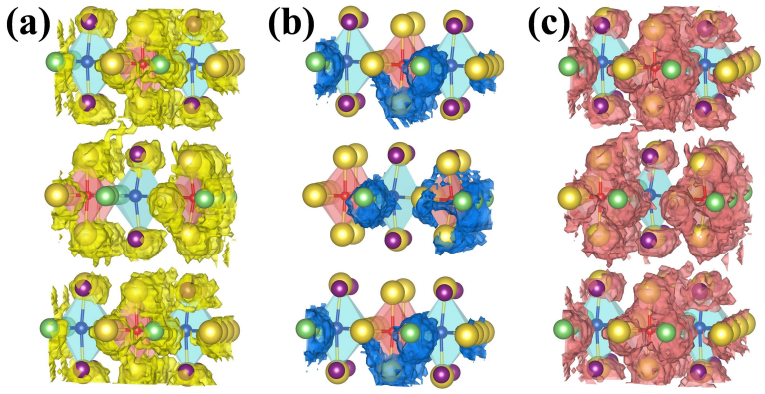

Fig. S8 (a) Na^+, (b) Li^+ and (c) the overall Na^+/Li^+ ion trajectories at 1000 K for $Na_3LiS_{0.5}O_{0.5}I_2$.

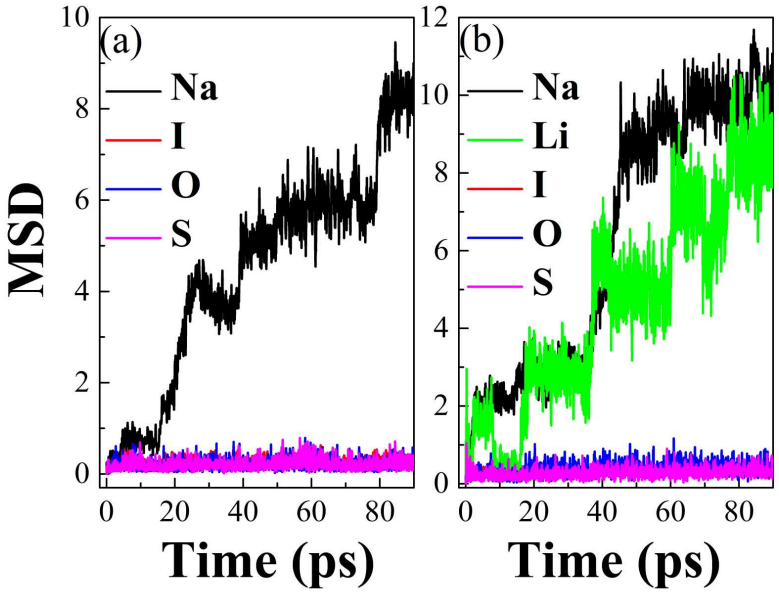

Fig. S9 Evolution of MSD for $Na_4S_{0.5}O_{0.5}I_2$ and $Na_3LiS_{0.5}O_{0.5}I_2$ at 1100 K, exhibiting long-range diffusion of alkali ions.

Table S1 Summary of potential candidates. The formation energy at 0 K (eV/atom) and critical temperature (T_c) to avoid phase decomposition into constituent compounds.

Compounds	USPEX	Phonon	Formation Energy	T_c
Na_4OI_2_139	√	**stable**	**＜0**	**＜438 K**
Na_4OCl_2_139	√	unstable	＜0	×
Na_4OICl_63	√	**stable**	**＜0**	**＜826 K**
Na_4OICl_129	√	unstable	＜0	×
$Na_4S_{0.5}O_{0.5}I_2$_65	√	**stable**	**＜0.025**	**>140 K**
Na_4SI_2_11	√	stable	＞0.025	×
Na_4SI_2_55	√	stable	＞0.025	×
Na_4SI_2_64	√	unstable	＞0.025	×
Na_4SICl_12	√	stable	＞0.025	×
Na_4SICl_8	√	stable	＞0.025	×
$Na_4S_{0.5}O_{0.5}ICl$_123	√	unstable	＞0.025	×
$Na_4S_{0.5}O_{0.5}ICl$_8	√	unstable	＞0.025	×

Table S2 Summary of High symmetry points in the Brillouin zone used in this paper.

High symmetry points	Coordinates
G	(0.00 0.00 0.00)
Z	(0.00 0.00 0.50)
T	(-0.50 0.00 0.50)
Y	(-0.50 0.00 0.00)
S	(-0.50 0.50 0.00)
X	(0.00 0.50 0.00)
U	(0.00 0.50 0.50)
R	(-0.50 0.50 0.50)
A	(0.50 0.50 0.50)
M	(0.50 0.50 0.00)